

Influence of pressure on fast dynamics in polyisobutylene

B. Begen^a, A. Kisliuk^a, V.N. Novikov^b, A.P. Sokolov^{a,*}, K. Niss^c,
A. Chauty-Cailliaux^c, C. Alba-Simionesco^c, B. Frick^d

^a University of Akron, Department of Polymer Science, 170 University Avenue, Akron, OH 44325-3909, USA

^b IA&E, Russian Academy of Sciences, Novosibirsk, 630090, Russia

^c Laboratoire de Chimie-Physique, UMR 8000, Université de Paris-Sud, 91405 Orsay, France

^d Institut Laue-Langevin, 6, rue Jules Horowitz, 38042 Grenoble, France

Available online 24 August 2006

Abstract

Influence of pressure on fast dynamics and elastic properties in polyisobutylene is studied using Raman, Brillouin and neutron scattering spectroscopy. Analysis of the results shows that the boson peak frequency increases with pressure stronger than the longitudinal sound velocity measured by Brillouin scattering. Moreover, the boson peak intensity decreases under pressure stronger in Raman scattering than in neutron scattering suggesting a decrease in the light-to-vibrations coupling coefficient $C(\nu)$. The strong decrease of the microscopic peak intensity under pressure in Raman spectra supports this suggestion. We argue that variations in $C(\nu)$ might be related to amplitude of structural fluctuations. We speculate that change in disorder and/or overall density under pressure is the main cause for the observed variations.

© 2006 Elsevier B.V. All rights reserved.

PACS: 63.50.+x; 64.70.Pf; 78.30.Ly

Keywords: Brillouin scattering; Neutron diffraction/scattering; Raman scattering; Glass transition; Pressure effects; Polymers and organics

1. Introduction

Understanding the microscopic nature of the fast dynamics in glasses (frequency range ν from ~ 1 GHz to ~ 3 THz) still remains a challenge. In crystals this region is dominated by acoustic vibrations, which show a Debye-like density of states ($g(\nu) \propto \nu^2$). However, two additional contributions have been observed in this frequency range for almost all glasses: (i) an anharmonic relaxation-like contribution that appears as a quasielastic scattering (QES) and (ii) a harmonic vibrational contribution which shows up as a broad so-called boson peak in light and neutron scattering spectra. The boson peak is associated with an excess density of low frequency vibrations over the expected Debye value. Despite many models suggested

for description of the fast dynamics [1–7], the nature of both kinds of excitations is still not clear.

It has been reported in many papers that the fast dynamics in glass forming systems is sensitive to sample preparation. In particular, quenching of glass-forming systems leads in most observations to an increase in the boson peak and QES intensities and to decrease of the boson peak frequency [8–12]. Application of external pressure has opposite effect: the boson peak intensity decreases and the frequency of the boson peak increases with pressure [13–17]. However, the systematic studies of this influence are very limited, although, they might help to understand better the microscopic nature of the fast dynamics through a comparison of experimental results to predictions of different models.

The present work analyzes the influence of pressure on fast dynamics and elastic properties of polyisobutylene (PIB) in the melt at room temperature and deep in the glassy state. It is shown that the Boson peak frequency

* Corresponding author. Tel.: +1 330 972 8409; fax: +1 330 972 5290.
E-mail address: alexei@uakron.edu (A.P. Sokolov).

increases under pressure stronger than the longitudinal sound velocity. We also observe that the variations of the boson peak intensity under pressure are stronger in Raman spectra than in the neutron scattering spectra suggesting a decrease of the so-called light-to-vibration coupling coefficient $C(\nu)$. The results are compared to variations of the fast dynamics under quenching.

2. Experimental

PIB with molecular weight $M_w \sim 20000$ (polydispersity ~ 1.04 , $T_g = 204$ K from DSC measurements) synthesized at the University of Akron was used in Raman and Brillouin scattering measurements. The sample was placed in a home-made optical moissanite pressure cell that was used to achieve the highest pressure $P \sim 1.8$ GPa. Ruby fluorescence was used to estimate the pressure in the cell. A reference ruby glued on the outer side of the cell and a mercury lamp were used for precise pressure analysis (accuracy better than ~ 0.05 GPa). Pressure variations were applied at room temperature. The pressure cell was placed in an optical Janis ST-100 model cryofurnace for temperature variations. The depolarized light scattering measurements were carried out in backscattering geometry at two temperatures, 295 K and 150 K, for each pressure. Raman spectra were measured using a Jobin Yvon T64000 triple-monochromator. The intensity of the spectra were normalized at high frequency modes, $\nu \sim 4\text{--}11$ THz. Polarized Brillouin scattering spectra were measured using the Sandercock tandem Fabry–Perot interferometer with free spectral range, FSR = 50 GHz.

The PIB sample used for the neutron scattering experiment had a molecular weight $M_w = 3580$ (polydispersity ~ 1.23) and was purchased from Polymer Standard Service. The samples used for neutron and light scattering have significantly different molecular weight. However, the M_w used is near the range where no changes in the Boson peak with molecular weight have been observed ($M_w > 4000$) [18,19]. Thus, a qualitative comparison of the neutron and light scattering data is justified. The sample was placed in clamp pressure cell with a hollow cylinder geometry and compression was applied in situ with 1.4 GPa as the maximum pressure. The pressure was applied in the melt (at 430 K) followed by subsequent cooling to 140 K. This procedure ensures that even for high pressure changes the sample was always in the melt. The experiment was performed at the time of flight instrument IN5 (ILL, Grenoble) using incoming neutrons with a wavelength of 5 Å and a resolution of FMHW = 103 μeV . The transmission of the sample was 88%, and about 93% of scattered intensity was incoherent contribution. The data were corrected for background, detector efficiency, absorption and self-shielding using the standard procedure (ILL program INX). No correction for multiple scattering was performed, but the data were considered only in the high Q -range where the multiple scattering effects are reduced. The data were then cor-

rected for the Debye–Waller factor and summed up over high angle detectors.

3. Results

The angle averaged dynamic structure factor obtained from the neutron scattering data at $T = 140$ K and corrected for the Debye–Waller factor is presented in Fig. 1 at different pressures. In the low energy range, the resulting spectrum is in good approximation proportional to $g(\nu)n(\nu, T)/\nu$, where $g(\nu)$ is the density of vibrational states and $n(\nu, T)$ the Bose temperature factor for energy gain side. The boson peak amplitude decreases and the frequency increases monotonously with pressure, in agreement with earlier studies on this and other materials. Fig. 2 shows

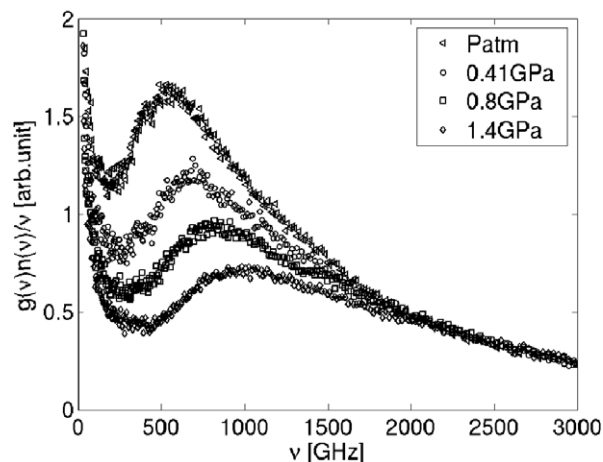


Fig. 1. Neutron scattering spectra of PIB at various pressures, $T = 140$ K.

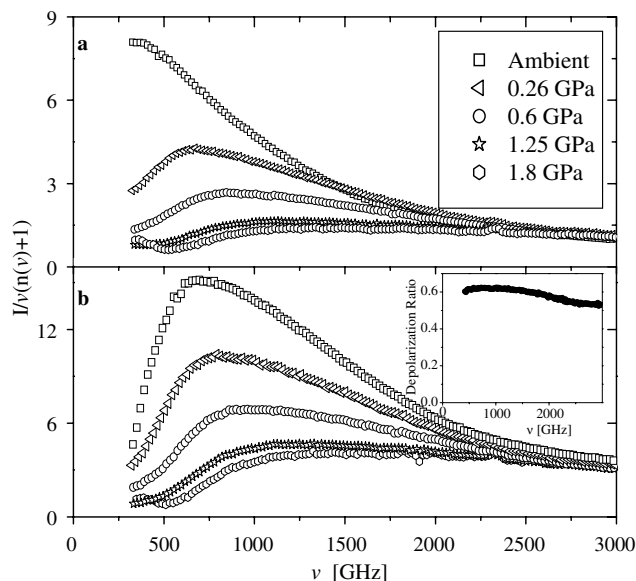


Fig. 2. Raman spectra of PIB at various pressures: (a) $T = 295$ K and (b) $T = 150$ K. Inset shows the depolarization ratio at 150 K and ambient pressure.

Table 1
Brillouin and boson peak frequency data at various pressures

Pressure	Temperature at 295 K		Temperature at 150 K	
	Brillouin peak frequency (GHz)	Boson peak frequency (GHz)	Brillouin peak frequency (GHz)	Boson peak frequency (GHz)
Ambient	15.36 ± 0.0005	353 ± 208	19.96 ± 0.0005	744 ± 45
0.26	22.01 ± 0.003	692 ± 129	22.98 ± 0.004	850 ± 73
0.6	25.28 ± 0.003	889 ± 187	26.51 ± 0.006	1030 ± 97
0.86	27.74 ± 0.006	1081 ± 214	29.03 ± 0.005	1124 ± 125
1.04	28.89 ± 0.008	1129 ± 296	30.13 ± 0.009	1231 ± 105
1.25	29.59 ± 0.004	1211 ± 218	30.32 ± 0.005	1327 ± 146
1.8	31.93 ± 0.007	1484 ± 392	32.81 ± 0.007	1652 ± 207

depolarized Raman scattering spectra presented as a spectral density, $I_n(\nu) = I(n)/\nu[n(\nu) + 1]$, where $[n(\nu) + 1]$ is the Bose temperature factor for the Stokes (energy loss) component. The boson peak is not clearly pronounced at ambient pressure and room temperature because of the strong QES contribution. At 150 K the boson peak is visible around 740 GHz even at ambient pressure. In both cases, as the pressure is increased, the boson peak intensity decreases and the peak frequency increases. However, the variations of the boson peak intensity appear to be smaller in the neutron scattering spectra (Fig. 1) than in the Raman scattering spectra (Fig. 2). For the quantitative analysis of the boson peak frequency, we used traditional approximation for the low-frequency Raman spectra [4]:

$$I_n(\nu) = \frac{A\nu_0}{\nu_0^2 + \nu^2} + B \exp \left\{ -\frac{[\ln(\nu/\nu_{BP})]^2}{2(W/\nu_{BP})^2} \right\} \quad (1)$$

where the first term describes the quasielastic contribution presented by a Lorentzian with width ν_0 and amplitude, A ; the second term describes the boson peak approximated by a log-normal function with the width W , amplitude B and the peak frequency ν_{BP} . The results of the fit show significant increase in the boson peak frequency with pressure (Table 1).

The Brillouin peak also shifts to higher frequencies under pressure (Fig. 3) indicating the change of the longi-

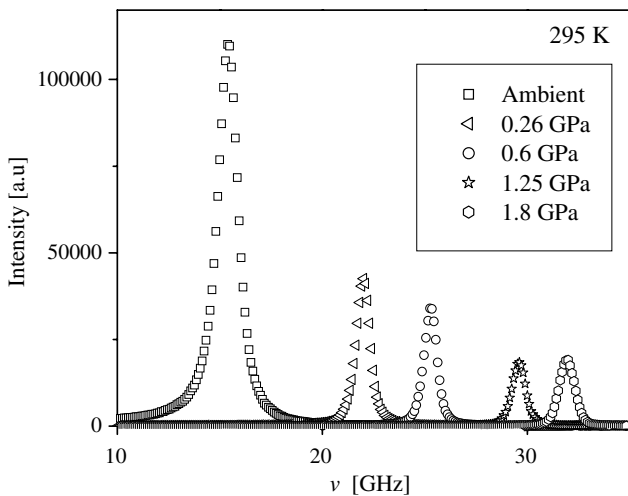


Fig. 3. Brillouin scattering spectra at various pressures, $T = 295$ K.

tudinal elastic modulus and density under compression. The frequency of the Brillouin peaks, ν_{Bril} , were estimated

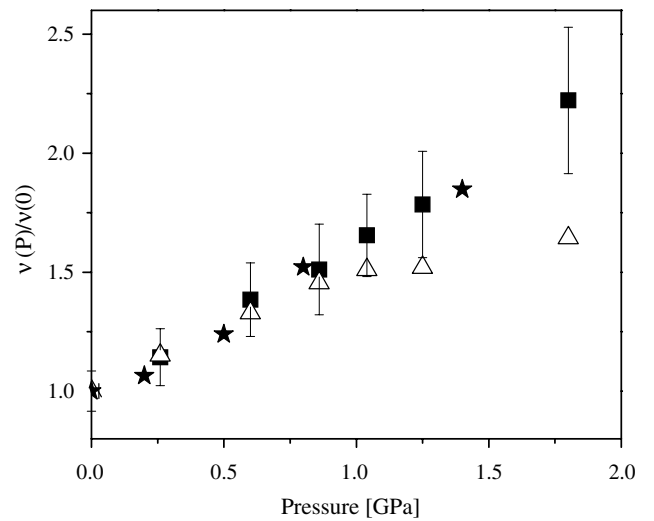


Fig. 4. Pressure dependence of the peak frequency normalized to the peak frequency at ambient pressure, $T = 150$ K: (Δ) polarized Brillouin peak, (\blacksquare) Boson peak measured by Raman scattering, (\star) Boson peak measured by neutron scattering.

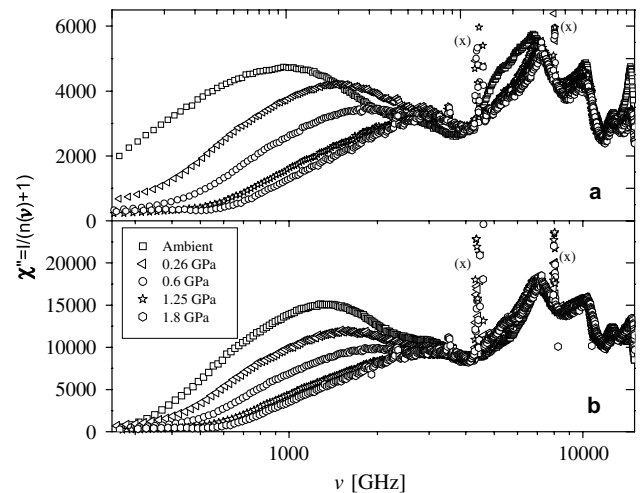


Fig. 5. Variations of the light scattering susceptibility spectra of PIB with pressure: (a) $T = 295$ K and (b) $T = 150$ K. (x) marks the Raman peaks of moissanite.

from the fit of the spectra by a Lorentzian (Table 1). It is known that the polarized Brillouin scattering appears due to scattering of light on longitudinal acoustic (LA) modes. The frequency of the peak is proportional to the LA-sound velocity, V_{LA} , $\nu_{\text{Bfil}} \propto V_{\text{LA}}$ (if one neglects variation in the refractive index). Comparison of the data normalized to their values at ambient pressure show that the boson peak frequency varies similar in neutron and Raman scattering and these variations are stronger than the shift of the Brillouin peak frequency especially at higher pressure (Fig. 4).

Fig. 5 presents the light scattering susceptibility spectra of PIB. A decrease in the intensity of the microscopic peak at $\nu \sim 1\text{--}3$ THz with increasing pressure is observed.

4. Discussion

The microscopic nature of the boson peak remains a subject of active discussions. Many models associate the boson peak with the existence of the intermediate range order and some correlation length in a glassy structure [1,15,20,21]. Duval et al. proposed a model [1], which attributed the origin of the boson peak to the vibrations localized in the nanoscale domains (blobs). In this model, $\nu_{\text{BP}} \approx aV/L$, here V is the sound velocity and L is the size of the blobs. Schirmacher and Maurer ascribe the boson peak to acoustic-like phonons strongly scattered by elastic constants fluctuations in disordered media [22]. In this model, the boson peak amplitude increases and the peak frequency softens with increase in the amplitude of the fluctuations. In the soft potential model (SPM) the boson peak corresponds to vibrations localized in soft atomic configurations [5,23]. Mutual interactions of these quasilocalized vibrations renormalize their bare spectrum to a universal form that well describes the boson peak [24]. In this model the amplitude of the boson peak is proportional to the number of the soft potentials that decreases with decrease of the force constant fluctuations.

Shift of the boson peak to higher frequencies under pressure has been reported in many earlier studies [13–15]. However, our analysis in Fig. 4 demonstrates that the variations of the boson peak frequency under pressure in both neutron and Raman spectra are stronger than the variations of the longitudinal sound velocity measured in the GHz frequency range at pressure above ~ 0.7 GPa. High depolarization ratio of the boson peak in PIB (inset Fig. 2(b)) and other polymers indicates transverse-like character of the vibrations contributing to the spectra at this frequency range. Thus, comparison of the boson peak shift to variations of transverse (shear) acoustic waves is more appropriate. The current studies do not provide measurements of TA Brillouin modes. However, it is known from studies of different materials including polymers that variations of TA modes under pressure are significantly smaller than that of longitudinal or bulk modes [15,25]. In the particular case of polystyrene (PS), the variations of the bulk modulus under pressure was ~ 1.5 times stronger than that of the shear modulus [25]. Thus, one expects an even larger differ-

ence in the pressure dependence for the transverse sound velocity and of the boson peak frequency. These expectations are supported by earlier studies of the boson peak variations under pressure in covalent glasses SiO_2 , GeO_2 and B_2O_3 [15]. Thus, a larger pressure variation in the boson peak frequency than in the sound velocity seems to be general for various kinds of glass forming systems. However, measurements of transverse Brillouin modes under pressure are required for more definitive conclusions.

It is also known that the boson peak varies under quenching and annealing of glasses [8–10,21] (although, we should mention that no variations in the neutron scattering spectra have been reported for quenched polybutadiene [26]). Quenching of glass forming materials leads to an effect opposite to the effect of pressure: the boson peak intensity increases and the frequency decreases with increase of the cooling rate [8–10,21]. Detailed studies of quenched barium-crown glass also demonstrate that variation of the boson peak frequency is stronger than the variations of the sound velocity measured using Brillouin scattering [9]. Thus, it appears to be a general observation that variations of the boson peak under pressure and/or thermal treatment are stronger than the variations of the sound velocity measured in the GHz frequency range. These results seem to contradict some models that suggest a linear relationship between the sound velocity and the boson peak frequency, though one should be careful with this conclusion because the variations of the sound velocity in the GHz frequency range might differ from the variations of the sound velocity in the THz frequency range. The latter is more relevant for the vibrations at the boson peak frequency. Inelastic X-ray scattering measurements under pressure can help to verify this suggestion.

Let us now turn to the analysis of the variations of the boson peak intensity under pressure. It is known that neutron scattering spectroscopy measures density of vibrational states, $g(\nu)$, directly. However, the Raman scattering intensity, $I(\nu)$, in disordered systems is proportional to the density of vibrational states multiplied by the light-to-vibrations coupling coefficient, $C(\nu)$ [20,27]:

$$I(\nu) = g(\nu)C(\nu)[n(\nu) + 1]/\nu \quad (2)$$

It has been shown theoretically that $C(\nu)$ for slightly damped acoustic waves should vary as $\sim \nu^2$ [20]. However, direct comparisons of the Raman spectra to inelastic neutron scattering data and to specific heat data have shown that $C(\nu)$ varies almost linearly with frequency around the boson peak [28–30].

The neutron and Raman scattering measurements (Figs. 1 and 2) show that the boson peak intensity decreases significantly with increasing pressure, consistent with other literature data. However, variations in the peak intensity appear to be stronger in light than in neutron scattering spectra. This observation clearly indicates a decrease in the light-to-vibrations coupling coefficient $C(\nu)$ under pressure. The light scattering susceptibility spectra (Fig. 5) show a shift to higher frequency and a decrease in the

intensity of the microscopic peak ($\nu \sim 1\text{--}3$ THz) under pressure. The microscopic peak is usually associated with the end of acoustic branch of the phonon spectra. The decrease of the microscopic peak intensity is another indication that $C(\nu)$ decreases with increasing pressure.

We want to emphasize that an increase of the boson peak intensity has been observed in many experiments on quenching glass forming systems [8–10,21]: the higher is the quenching rate the higher is the amplitude of the boson peak. Comparison of the Raman and neutron scattering data on quenched chalcogenide glass reveals that the intensity increases stronger in the light than in the neutron scattering spectra [8], suggesting that quenching leads to an increase in $C(\nu)$.

Although, the microscopic description of $C(\nu)$ in disordered materials still does not exist, it is obvious that at these frequencies $C(\nu) \sim 0$ in ordered structures (crystals) and it should increase with increase in disorder of the system. Qualitatively, such behavior of the coupling coefficient is easy to understand. Due to wave-vector conservation rule, $C(\nu)$ for plane-wave phonons is non-zero only at Brillouin frequencies. It became non-zero at other frequencies because of deviation of the phonon wave-function from a plane wave. This deviation is caused by density and elastic constants fluctuations. So, a decrease in the amplitude of the fluctuations should lead to a decrease of the coupling coefficient $C(\nu)$. A semi-quantitative analysis of the influence of the static disorder on the boson peak amplitude and light-to-vibration coupling coefficient can be performed within the spatially damped plane waves model. In this model vibrations are described by distorted plane waves $u_Q(\mathbf{r}) \propto \exp(i\mathbf{Q}\mathbf{r} - r/l)$ that have a finite mean free path $l(Q)$. The latter might be related to the static fluctuations of the elastic constants and density via the mean square fluctuation of the sound velocity, ΔV , as

$$l^{-1}(Q) \sim 8R_c^3 Q^4 \langle (\Delta V/V)^2 \rangle, \quad (3)$$

here R_c is the spatial correlation length of the fluctuations [31]. Using the model of spatially damped plane waves, it was shown that $C(\nu)$, defined by an integral

$$C(\nu) \propto \int d^3R d^3r \langle \nabla u_Q(\vec{R}) \nabla u_Q(\vec{R} + \vec{r}) \rangle, \quad (4)$$

is proportional to $l^{-1}(Q)$ [32,33]:

$$C(\nu) \propto \frac{l^{-1}}{Q^2 + l^{-2}} \quad (5)$$

for a correlation length longer than the vibration wavelength, $C(\nu) \propto l^{-1}(Q)/Q^2$. Using the assumption (Eq. 3), we arrive to the qualitative relationship, $C(\nu) \propto R_c^3 \langle (\Delta V/V)^2 \rangle$. Thus, the coupling constant should decrease with a decrease in the amplitude of the sound velocity fluctuations.

External pressure as well as quenching of glass forming liquids leads to change of average parameters (density, elastic moduli) and amplitude of their fluctuations. The

observed change of the amplitude of the boson peak may be related to variations of both, average values (e.g., an increase of the sound velocity leads to a decrease of the density of states for acoustic-like vibrations) and amplitude of their fluctuations. However, the light-to-vibrations coupling coefficient should be more sensitive to amplitude of the sound velocity fluctuations than to variations of the average values (Eqs. (3)–(5)). We speculate that the system becomes more homogeneous (the amplitude of elastic constants and density fluctuations decreases) under high pressure while quenching of the glass forming systems increases the amplitude of frozen in fluctuations. These variations lead to change in $C(\nu)$ through the changes in vibrational $l(Q)$. However, we cannot exclude that the observed variations in $C(\nu)$ might be caused by a decrease in the averaged value of the Pockel's coefficients (acousto-optical constants) and more detailed studies are required to disentangle this problem.

In Ref. [34] it was shown that a decrease of $l(Q)$ leads to an increase of the excess low-frequency density of acoustic-like vibrational states, i.e., to an increase of the boson peak amplitude. More thorough theoretical consideration presented in [22] predicts the increase of the boson peak intensity and decrease of its frequency with the increase in amplitude of the sound velocity fluctuations. Our analysis shows that the change in the boson peak frequency is coupled to the change of its intensity in the way predicted by the model, i.e., increase of disorder (quenching) leads to decrease of the boson peak frequency and increase of its amplitude while suppression of fluctuations (high pressure) leads to opposite effect. We want to emphasize that our results might be consistent with other models suggested for description of the boson peak (e.g., recently proposed [35]). More detailed comparison of our data to predictions of various models is forthcoming.

5. Conclusions

Variations of the fast dynamics in PIB under pressure have been analyzed using Raman, Brillouin and neutron scattering techniques. The analysis revealed that the boson peak frequency varies stronger than the sound velocity and the intensity of the boson peak varies stronger in light than in neutron scattering spectra. The latter indicates a decrease of the light-to-vibrations coupling coefficient $C(\nu)$ under pressure. The observed changes in $C(\nu)$ might be ascribed to a decrease of disorder or decrease of heterogeneity in densified glassy structure. These data combined with earlier results on quenched glasses provide a consistent picture: increase in disorder and/or decrease in density leads to a decrease of the boson peak frequency and an increase in its amplitude.

Acknowledgments

Akron team thanks the National Science Foundation for the financial support (Grants DMR-0315388 and INT-0129082).

References

- [1] E. Duval, A. Boukenter, T. Achibat, *J. Phys.: Condens. Matter* 2 (1990) 10227.
- [2] T.S. Grigera, V. Martin-Mayor, G. Parisi, *Nature* 422 (2003) 289.
- [3] S.R. Elliot, *Europhys. Lett.* 19 (1992) 201.
- [4] V.K. Malinovsky, V.N. Novikov, A.P. Sokolov, *Phys. Lett. A* 153 (1991) 63.
- [5] V.L. Gurevich, D.A. Parshin, J. Pelous, H.R. Schober, *Phys. Rev. B* 48 (1993) 16318.
- [6] C.N. Taraskin, S.R. Elliott, *Phys. Rev. B* 59 (1999) 8572.
- [7] D. Quitmann, M. Soltwisch, G. Ruocco, *J. Non-Cryst. Solids* 203 (1996) 12.
- [8] S.L. Isakov, S.N. Ishmaev, V.K. Malinovsky, V.N. Novikov, P.P. Parshin, S.N. Popov, A.P. Sokolov, M.G. Zemlyanov, *Solid State Commun.* 86 (1993) 123.
- [9] C. Levelut, N. Gaimes, F. Terki, G. Cohen-Solal, J. Pelous, R. Vacher, *Phys. Rev. B* 51 (1995) 8606.
- [10] C.A. Angell, Y. Yue, L. Wang, J.R.D. Copley, S. Borick, S. Mossa, *J. Phys.* 15 (2003) S1051.
- [11] E. Duval, L. Saviot, L. David, S. Etienne, J.F. Jal, *Europhys. Lett.* 63 (2003) 778.
- [12] C. Chemarin, B. Champagnon, G. Panczer, *J. Non-Cryst. Solids* 216 (1997) 111.
- [13] B. Frick, C. Alba-Simionesco, *Appl. Phys. A* 74S549 (2002).
- [14] M. Yamaguchi, E.L. Chronister, *Recent Res. Dev. Non-Cryst. Solids* 2 (2002) 191.
- [15] J. Schroeder, W. Wu, J.L. Apkarian, M. Lee, L. Hwa, C.T. Moynihan, *J. Non-Cryst. Solids* 349 (2004) 88.
- [16] S. Sugai, A. Onodera, *Phys. Rev. Lett.* 77 (1996) 4210.
- [17] G.E. Walrafen, Y.C. Chu, M.S. Hokmabadi, *J. Chem. Phys.* 92 (1990) 6987.
- [18] Y. Ding, V.N. Novikov, A.P. Sokolov, A. Cailliaux, C. Dalle-Ferrier, C. Alba-Simionesco, B. Frick, *Macromolecules* 37 (2004) 9264.
- [19] B. Frick, G. Dossseh, A. Cailliaux, C. Alba-Simionesco, *Chem. Phys.* 292 (2003) 311.
- [20] A.J. Martin, W. Brenig, *Phys. Status Solidi B* 64 (1974) 163.
- [21] V.K. Malinovsky, A.P. Sokolov, *Solid State Commun.* 57 (1986) 757.
- [22] E. Maurer, W.J. Schirmacher, *Low Temp. Phys.* 137 (2004) 453.
- [23] V.G. Karpov, M.I. Klinger, F.N. Ignat'ev, *Zh. Eksp. Teor. Fiz.* 84 (1983) 760; V.G. Karpov, M.I. Klinger, F.N. Ignat'ev, *Sov. Phys. JETP* 57 (1983) 439.
- [24] V.L. Gurevich, D.A. Parshin, H.R. Schober, *Phys. Rev. B* 67 (2003) 094203.
- [25] D.S. Hughes, J.L. Kelly, *Phys. Rev.* 92 (1953) 1145.
- [26] R. Zorn, B. Frick, *J. Chem. Phys.* 108 (1998) 3327.
- [27] R. Shuker, R. Gammon, *Phys. Rev. Lett.* 25 (1970) 222.
- [28] A.P. Sokolov, A. Kisliuk, D. Quitmann, E. Duval, *Phys. Rev. B* 48 (1993) 7692.
- [29] N.V. Surovtsev, A.P. Sokolov, *Phys. Rev. B* 66 (2002) 054205.
- [30] A.P. Sokolov, U. Buchenau, W. Steffen, B. Frick, A. Wischnewski, *Phys. Rev. B* 52 (1995) R9815.
- [31] J.E. Graebner, B. Golding, L.C. Allen, *Phys. Rev. B* 34 (1986) 5696.
- [32] J. Jäckle, K. Frobose, *J. Phys. F* 9 (1979) 967.
- [33] L. Saviot, E. Duval, N. Surovtsev, J.F. Jal, A.J. Dianoux, *Phys. Rev. B* 60 (1999) 18.
- [34] A.P. Sokolov, R. Calemczuk, B. Salce, A. Kisliuk, D. Quitmann, E. Duval, *Phys. Rev. Lett.* 78 (1997) 2405.
- [35] V.L. Gurevich, D.A. Parshin, H.R. Schober, *Phys. Rev. B* 71 (2005) 14209.